Annual Technical Report
on
PROTEIN CRYSTAL GROWTH IN LOW GRAVITY
NASA #NAG8-774
CMR-91-4
SPO#7218
for the period
June 6, 1990 through June 5, 1991

Submitted to
George C. Marshall Space Flight Center
ES-76, Space Science Lab
MSFC, AL 35812

Principal Investigator:

Robert S. Feigelson, Professor (Res.)
Center for Materials Research
Stanford, California 94305-4045
(415) 723-4007

October 1991

TABLE OF CONTENTS

ABSTRACT

This report covers the period of June 6, 1990 to June 5, 1991 for NASA Grant NAG 8-774. The objectives of and approach to the research is outlined. The application graphoepitaxy (artificial epitaxy) to proteins is detailed. The development of a method for the control of nucleation is discussed. The factor affecting the morphology of isocitrate lyase crystals are presented

I. INTRODUCTION

The objective of this research is to study the effect of low gravity on the growth of protein crystals and those parameters which will affect growth and crystal quality. The proper design of the flight hardware and experimental protocols are highly dependent on understanding the factors which influence the nucleation and growth of crystals of biological macromolecules. Thus, the primary objective of this research is centered on investigating those factors and relating them to the body of knowledge which has been built up for "small molecule" crystallization. This data also provides a basis of comparison for the results obtained from low-g experiments.

The main component of this research program is the study of mechanisms involved in protein crystallization and those parameters which influence the growth process and crystalline perfection. Both canavalin and lysozyme are being used as the basic model proteins in these studies. Other biological macromolecules such as isocitrate lyase have been included in this research program when they provide an opportunity to better understand the nature of the crystallization process. The program involves four broad areas:

1. The application of both classical and novel chemical and physical techniques to study the fundamentals of protein crystallization. Included in this area are the study of the phase relationships in the systems of interest, primarily the factors controlling solubility, the study of growth kinetics to determine the growth rate controlling mechanism and the relevant activation energy involved in the process. The effects of fluid flow on the growth and perfection of protein crystals will be studied using flow visualization techniques. The use of electrochemical techniques to monitor and/or control crystallization will be studied also. The effects of applied

voltages on nucleation and growth are not known nor is the magnitude of the potentials which may develop on the crystal during growth.

2. Characterization of protein crystals. Optical microscopy will give a general evaluation of crystal morphology, size and perfection. Phase contrast techniques will give enhanced contrast to the surface features allowing observation down to the 0.1μ level. For more detailed surface imaging the application of Scanning Tunneling Microscopy and Atomic Force Microscopy to protein crystals will be investigated. To study the defects occurring in the bulk of the crystals, the applicability of Synchrotron x-ray topography will be studied. The characterization studies will be attempting to associate the defects in protein crystals with the growth conditions to develop insights for growing crystals of greater perfection.

3. Control of nucleation and growth. The information developed in the phase relationship studies of section (1) will be used to design experiments to separately control the nucleation and growth processes. The information from section (2) will be used to optimize the growth.

4. The design and construction of a prototype of space flight hardware. The design will incorporate the results of section (3) and will be instrumented to gather the types of data that have been acquired in the ground based studies.

II. GRAPHOEPITAXY

The widely used hanging (or sitting) drop vapor diffusion technique[1] for protein crystal growth is not completely satisfactory. The growth of any crystal from solution without seeding requires that a critical nucleus be formed which, in turn, requires that the critical supersaturation be exceeded.[2] This critical supersaturation is in excess of that which is necessary for well-controlled growth and it leads to two effects: multiple nucleation of many small crystals and/or rapid growth leading to poor quality crystals. In addition, gravity usually causes the crystals to settle in the drop, resulting in clusters of misoriented crystals which are unsuitable for structure determinations.

A preliminary study on the use of graphoepitaxy (artificial epitaxy) to grow oriented crystals of the proteins catalase, lysozyme and canavalin has been completed. Graphoepitaxy employes a substrate patterned on a micron scale to induce an orientation to the growing crystals. While the basic technique has been used for the growth of inorganic crystals consisting of small molecules,[3] this study is the first successful application of artificial epitaxy to the growth of protein crystals. The closest previous work is that of McPherson and Shlichta[4,5] in which protein crystals were grown on minerals.

The substrates for the growth of the protein crystals in this study were single-crystal (100) -, (111) - or (211) - silicon (Si) wafers. A striated microrelief (5 μm+ 5 μm period, 1-2 μm depth grooves) was prepared on these substrates by anisotropic etching so that the grooves were bounded by closely-packed (111) - faces typical of diamond-like crystals. The striations had defined crystallographic directions: <110> and <100> on the (100) - substrates, <110> and <211> on the (111) - substrates, and <110> on the (211) - substrates. In addition, a regular two-dimensional array of hexagonal holes about 6 μm across and 1 μm in depth and 15 μm center-to-center distances were created on the (111) - substrates. After the microrelief was made, some of the substrates were thermally oxidized so that they were coated by an amorphous SiO_2 layer 0.3 - 0.4 μm in thickness. In a given experiment, both oxidized and non-oxidized substrates were used.

All crystallizations were carried out at room temperature by variations of the vapor diffusion method.[6] In the case of catalase and lysozyme, crystals were grown in a Petri-dish-based apparatus commonly used for protein crystallization.[6] Substrates were placed on a pedestal and a peripheral well was filled by a precipitant solution. In the case of canavalin, crystals were grown in a plastic box (Crystal Plate) produced by Flow Laboratories for the crystallization of proteins. The crystallizing solution for catalase was prepared from catalase penicillum microfungus octale, mol. weight 300,000 (300 kDa). A fine-crystalline catalase suspension prepared according to[7] was centrifuged for 40

minutes at velocity 8,000 rpm and the precipitate was dissolved in 0.05M sodium acetate buffer solution, pH 5.2, containing 0.5M ammonium sulfate. The solution containing 10 to 20 mg/ml of the catalase was centrifuged just before crystallization and 5 to 10 μl droplets of the solution were pipetted onto the substrates. The precipitant solution was usually 1.4M ammonium sulfate. In some experiments, an initial precipitant solution contained only 0.8M ammonium sulfate and the concentration was gradually increased up to 1.4M by introducing the sulfate via a hole in the top cover of the crystallization chamber.

The crystallization solution for canavalin contained canavalin (30 mg/ml) dissolved in a pH 9.2 (ammonium hydroxide) solution with 1% sodium chloride (NaCl) added. In some experiments, detergents such as n-octyl β-D-glucopyranoside (β-octylglucoside, β-OG) and sodium dodecyl sulfate (SDS) were used. Both were found to be effective in the sense that more small crystallites were formed As a counter-solution, an acetic acid (HAc) solution with pH between 5 and 6 was used. It was found that, at pH = 4, crystallization was uncontrollable, leading to precipitates, while at pH = 7 no crystallization occurred in a reasonable length of time (1 week). Three configurations were used for crystallization: standing droplet, hanging droplet (on a glass substrate without microrelief), and a droplet "sandwiched" between the substrate and the cover glass plate. The sandwiched droplet was the most effective for the crystallization of canavalin. This configuration also gave some insights into the features inherent in crystallization of proteins by artificial epitaxy.

The crystallizing solution for lysozyme was made from a buffer solution containing 30 mg/ml lysozyme, 0.1 M sodium acetate (pH 4) with an equal volume of a 8% NaCl solution added so that the final solution concentrations were 15 mg/ml lysozyme and 4% NaCl. As a counter-solution, NaCl solutions with concentrations of 8% or 14% were used. The 8% solution did not give any results in a week's time, while with the 14% solution the first crystals appeared (as was observed at 100 x) in a day.

In situ-optical microscopy at magnifications from 50 x to 100 x was used to observe the growing crystal. All crystals studied were transparent, which allowed the micro-relief to be seen through them and thus it was possible to make conclusions on orientation effects.

The most valuable results were of a morphological nature and consisted of a comparison of crystallite orientation (their principal elements such as edges, diagonals, etc.) with respect to the microrelief.

As was noted above, the catalase crystals were grown in droplets. In this case, wetting of the substrate by the solution was moderate so that the contact angles of the droplets had some value between 60° and 90° C. Accordingly, the density of the crystal

deposition on the substrate was different for different areas under a given droplet, being higher at periphery, where supersaturation (as a result of evaporation of the solvent) is larger, and lower in the central part of the droplet. In both regions, the majority of crystals grew with their edges parallel to the substrate striations (Fig. 1). In addition to the edge-parallel-to-striations orientation, sometimes the diagonals of the crystals were parallel to the striations (Fig. 2). Once deposited, the catalase crystals remained immobile and continued to grow preferentially in width, but also in height and in depth.

Fig. 1. Catalase crystals deposited at relatively low supersaturations.

Important information about growth of catalase crystals on substrates with micro-relief is obtained by the investigation of the morphology of the face of the crystals resting on the substrate (backside morphology). Figure 3 shows the backside morphology of a crystal which was first mechanically detached from the substrate and then overturned. The rib-type structure of the backside indicates that the crystal had grown into the micro-relief after it was attached to the substrate. A similar behavior was also observed for canavalin crystals (see below).
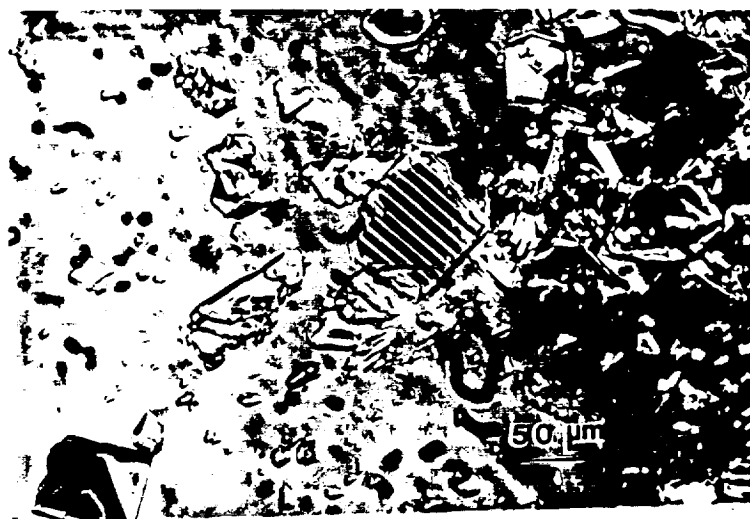
Fig. 2. Diagonal of orientation.

Fig. 3. Backside of a catalase crystals removed from the substrate. Note parallel striation (with a period equal to that of striated micro-relief) as a result of the crystal growing into the substrate after a long period of time (about 3 days) in a supersaturated solution.

One of the results obtained in this study was on the effect of reliefs of different symmetry and/or different profiles on the orientation of the crystals. The ratio of the number of oriented-to-nonoriented crystals in a given droplet in a given area, can serve as a quantitative measure of this effect. Based on such a measurement, the best orientation of catalase crystals was achieved, first, with striated micro-reliefs as opposed to the hexagonal-type holes, and, secondly, with the striated reliefs on <100> - striped (100) - substrates and on (211) - substrates (<110> stripes), as opposed to other directions of striations. For example, with <110>/(100) substrates, about 80% of crystals had their edges parallel to the striations. The advantage of the striated relief was evidently connected with the principle morphology of catalase crystals, namely with the existence of rather distinctive edges (the crystals are bounded as a rule by simple rhombohedral faces with only two of six faces being visible, while the other four faces form very narrow stripes).

In respect to the orientation relationships, it must be noted that although hexagonal-shaped pits were not effective for oriented crystallization, sometimes catalase crystals were oriented with their edges parallel to rows of the hexagonal pits.

The orientation mechanism(s) will be discussed in more detail below in relation to the data on canavalin and lysozyme crystals.

Canavalin crystals were also oriented on substrates with micro-relief and again striated relief was most effective. This is to be expected since canavalin crystals have a rhombohedral shape with rather sharp edges (see Fig. 1)[8] under the growth conditions employed in this study.

Figure 4 demonstrates the effect of the micro-relief which orients many (although not all) of the crystals.

As was noted above, the crystals were obtained in a "sandwich" system where solution can move . At least three events are inherent in such a system: a) crystals formed can change their orientation and position during relatively short time intervals, b) the crystals can be overturned, c) the crystals are often removed from the substrate to surrounding areas of solution.

The first type of event involved both movement from nonoriented-to-oriented and from oriented-to-nonoriented positions (sometimes also from one nonoriented to another nonoriented one). The changes were most remarkable for relatively small crystals, especially for relatively thin ones. On the other hand, the smallest (of the visible) crystallites which fill a single groove were as a rule in oriented positions even though they sometimes moved. This indicated that it might be possible to ensure better orientation by initially growing more small crystals. To test this, detergents such as β-OG and SDS were

added to the crystallization solutions and, in fact, were found to be effective. The crystals formed were in general smaller in size.
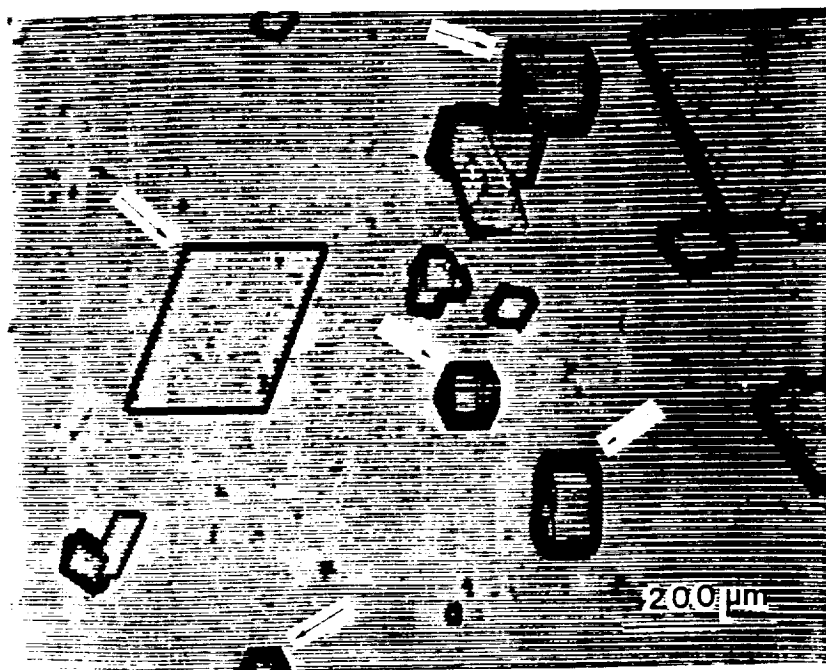

Fig. 4. Crystals of canavalin oriented parallel to striations (as indicated by arrows) together with crystals having different orientations.

Another feature observed in the sandwich version was the overturning of crystals. The period of the striations on the backside of overturned crystals was exactly equal to the period (groove plus hill) of the micro-relief. This confirmed that the backside morphology was a result of the crystal growing into the substrate during the first stage of their formation. The overturned crystals had striations parallel to both their edges and their diagonal, as well as non-parallel to any distinctive direction. The first two cases (parallel to edges and to diagonal) once again illustrates the effect of the relief in orienting the crystallites.

Only some preliminary results on artificial epitaxy were obtained with lysozyme. As is seen in Fig. 5, these crystallites have some of their edges parallel to the substrate striations as a demonstrating deposition orientation .

It is possible to distinguish at least five different orientation mechanisms operative in artificial epitaxy. These mechanisms, which can operate both separately and simultaneously[3,9] include: a) orientation by means of topographic micro-relief

10

("macroscopic Kossel-Strankei mechanism"), b) orientation under action of capillary forces, c) orientation by periodic thermal relief (in directional solidification of a melt), d) orientation by symmetric anisotropic deformation (mainly for solid-state crystallization), and e) orientation by cooperative rotations of crystals.

Fig. 5.   Lysozyme crystals deposited in orientation positions with respect to striated micro-relief.

In the case of protein crystallization from solution, mechanisms (a), (b) and (e) could be operative. However, under conditions typical for these experiments, mechanism (e) which operates mainly at the stage of coalescence of crystals should be excluded. Mechanisms (a) and (b) remain and our results, as described above, indicate that both of these mechanisms are active.

In the figures presented, the oriented crystals are confined by the stripes, which supports the topographic mechanism. At the same time, there are many indications (especially with canavalin) that capillary forces are active in the orientation of the crystals. Among these are the phenomena of the "mooring" of relatively small crystals with larger ones and the orientation of the smallest (visible) crystals with the relief. The latter fact is worth a more detailed discussion. It is difficult to imagine that all these small crystals have a width exactly equal to the width of the relief grooves. Most probably, the crystals have a

width smaller than that of the grooves and they take a symmetric position in respect to the grooves' wall due to the capillary mechanism.[10] Thus, based on the experimental results, a combined orientation mechanism including both topographic and capillary effects is operative in this case.

The action of detergents has an effect on these processes. When the protein solution with the detergent was placed on a substrate as a droplet, far better wetting (in comparison with a "normal" solution without detergent) was observed. This "macroscopic" effect is evidently related to molecular interactions in the solution facilitating, first, the formation of a large number of small crystallites and, second, the mobility of the crystallites in the solution. The mechanisms of the effect remain unclear.

The issue of initial stages of protein crystallization is of principal importance. In general, the specifics of protein crystallization in comparison with the classic ("small-molecule") crystal growth was discussed by Feigelson.[11] It is clear that in view of the role of the medium (in particular of water molecules) in formation of protein crystals, nucleation here is a far more complicated process than that for usual (small-molecule) materials. Nevertheless, for proteins, similarly to small-molecule materials, it is possible to distinguish between homogeneous and heterogeneous nucleation. In particular in our experiments, we were able to note a role of foreign particles in nucleation (at least for lysozyme). We compared three cases: when the crystallization solution was filtered (0.5 μm filter), when it was centrifuged, and when no special pretreatment was done. At some relatively small supersaturations in the centrifuged and untreated solutions, the first observable crystals appeared in a day (100 x optical microscope) and there were a large number of crystals which were nonoriented. Under the same conditions, in the filtered solution, the first crystals appeared in a week. Growth was rather sluggish and many of the crystals were oriented in respect of the micro-relief. In general, it was noted that the relief was rather active in causing crystallization. In a droplet covered area, with and without relief, nucleation under the same conditions occurred far more readily on the relief. This means that the "artificial lattice" inherent in artificial epitaxy (graphoepitaxy) serves as a heterogeneous catalyst for nucleation. In this respect, some comments should be made on the results of McPherson and coworkers concerning the heteroepitaxial growth of proteins on single-crystalline (mineral) substrates.[4,5] The authors reported the oriented growth of lysozyme on apophyllite, noting the relationship of lattice parameters of the two materials as it is considered in classic heteroepitaxy. An alternative explanation of their results can be found in the principles of artificial epitaxy. Macroscopic (more than one-monolayer-height), oriented steps can be present on cleaved or natural faces of crystals such as the minerals used in McPherson's experiments. These steps can, in principle,

orient depositing crystals, especially if the crystals are relatively large as in the case of protein crystallization.

Finally, it should be noted that our experiments on oxidized and non-oxidized Si substrates have shown no difference in results, indicating that no orienting effects from single-crystalline substrates ("classic heteroepitaxy") take place.

SUMMARY

The results of these preliminary studies show that in the case of catalase, lysozyme and canavalin graphoepitaxy does cause orientation of the growing crystals. In most cases, the orientation is such that an edge of the growing crystal is parallel to the relief. In a few instances, the orientation is along the face diagonal of the growing crystal. The amount of misorientation between individual macroscopically oriented crystals is not known, but it is probably small. A cluster of such macroscopically oriented crystals which had grown together could yield preliminary structural data.

The orientation of the growing crystals is the result of two mechanisms. The first mechanism is a morphological one in which the edge of the crystal attaches the the wall of edge of the relief. Smaller crystals are oriented within the relief by capillary forces. Both mechanisms may be active during growth.

There is evidence to suggest that the patterned substrates induce nucleation at lower supersaturation than would be necessary without the substrate. This is advantageous because, as was previously mentioned, it limits the number of nuclei and provides a slower growth rate which can lead to better crystals. In some cases (Fig. 4), large (100 to 200 μ) crystals grow in isolation. These crystals can be used as seeds in one of two ways. If the space around the crystal is large enough, more nutrient solution can be added and the crystal grown out to a size suitable for diffraction studies. If there is not enough space to allow additional growth, the substrate can be cleaned of extraneous crystals and the seed grown to the desired size. The presence of the substrate facilitates the handling of the seed crystals.

III. CONTROL OF NUCLEATION

It is well known that crystal growth involves two separate processes; 1) nucleation of the species desired, and 2) the growth of these nuclei into macroscopic crystals of suitable size and quality for the intended application. Nucleation involves a phase transformation in which a solid surface of the phase desired is created within a nutrient phase. The crystal growth process, on the other hand, involves heat and mass transport, i.e. removing the latent heat evolved during the crystallization process and supplying nutrient to the growing crystal at an appropriate rate. It is not surprising, therefore, that the energetics involved in these two processes are not the same. In many cases, they are significantly different.

It is of practical importance to be able to isolate and control the nucleation process separately from the subsequent growth phase. In small molecule crystal growth, this is most often accomplished by introducing an appropriate seed crystal (usually of the material being grown) into a melt, vapor, or solution. The use of a seed by-passes the nucleation stage by providing the solid-liquid interface necessary for the crystal growth process to proceed. In the growth of crystals containing biological macromolecules, obtaining seeds of the appropriate size and quality is often very difficult and has rarely been an attractive strategy. In most macromolecular crystal growth processes currently in use, the nucleation step is achieved in the growth solution under poorly understood conditions and the growth proceeds in a more or less uncontrolled manner.

In crystal growth from aqueous solutions, (the principal, if not only method, for growing crystals of biological species) the driving force of nucleation is the supersaturation. The supersaturation, c/s, where c is the actual solution concentration and s is the concentration at the saturation point, provides the excess energy needed to form the solid surface in the solution phase (homogeneous nucleation). The temperature-composition diagram in Fig. 6. illustrates the relationship between solubility and supersaturation. The solid line is the solubility curve, which divides the diagram into two regions: unsaturated and supersaturated. A second curve, the supersolubility curve, divides supersaturated region into labile and metastable regions. The labile region is unstable and nuclei form readily by spontaneous fluctuations in composition. Solutions are quite stable in the metastable state and it is only in this region where controlled crystal growth is possible.[12] The width of the metastable region depends on a number of factors, including purity of the starting materials. The supersaturation needed for homogeneous nucleation is often significantly greater than that needed for growth and that is why, after the initial nuclei are formed, growth normally proceeds in a rapid uncontrolled manner.

14

The supersaturation necessary for nucleation can often be reduced if a foreign substance is present upon which the species of interest prefers to nucleate (heterogeneous nucleation).
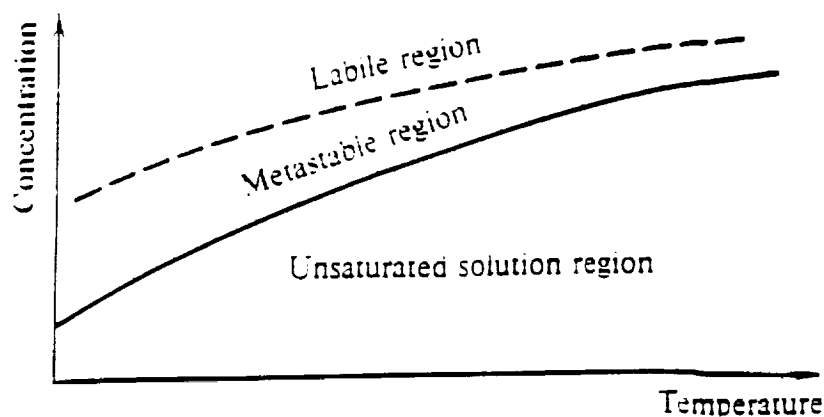

Fig. 6.   Schematic diagram of solubility for a substance whose solubility increases with temperature.

Starting from an undersaturated condition, the metastable region can be reached in principle by either changing temperature at constant composition or composition at constant temperature. Most biological macromolecular crystals are grown by the latter technique because the temperature dependent coefficient of solubility (phase equilibria) is usually not known and, in some cases, is negligible. In Fig. 7, the phase diagram for canavalin is given showing regions of both temperature dependent and independent solubility.[13]

With respect to both nucleation and growth processes, temperature change methods are usually easier to control with more precision than other techniques such as evaporation and therefore, if possible, would be the method of choice.

One method for controlling nucleation without using seeds involves the localized control of supersaturation in a specific region of a near-saturated bulk solution. By doing so, nucleation will be confined to a small volume of the solution and the number of crystallites which form will thus be severely limited. With the bulk of the solution near or just at saturation, the crystals nucleated can then be grown in a controlled manner by changing the solution temperature and hence the bulk supersaturation.

Localized nucleation can be accomplished by controlling temperature or solute concentration in that region. In the work discussed here, the localized supersaturation is controlled by controlling the temperature in an approximately 0.4 mm^3 region of a >1 cm^3 protein solution. The steep temperature gradients developed can therefore restrict nucleation to a very small volume of the overall solution. An illustration of the process is given in Fig. 8.
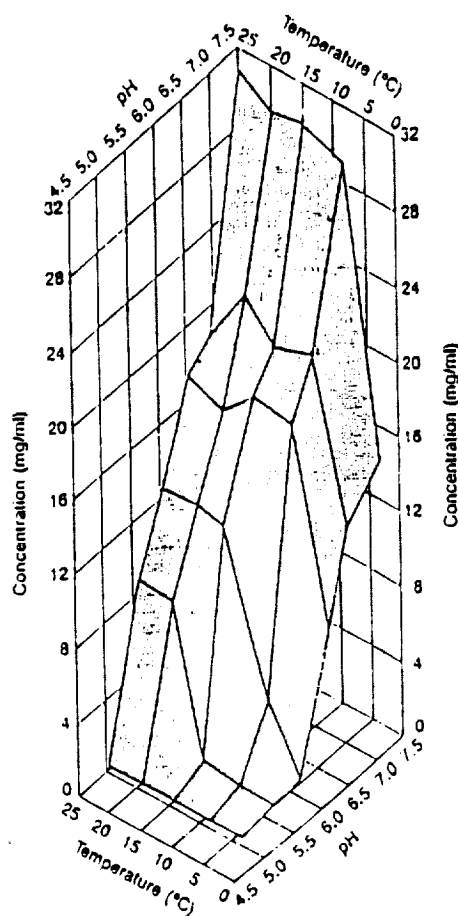
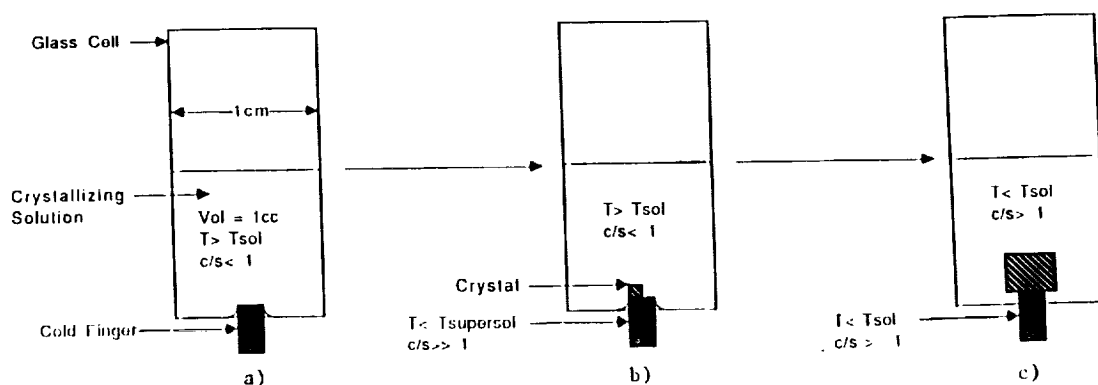Fig. 7. Solubility diagram for canavalin showing dependence on temperature and pH.[13]

Fig. 8. Controlled nucleation using temperature control method (thermonucleation).
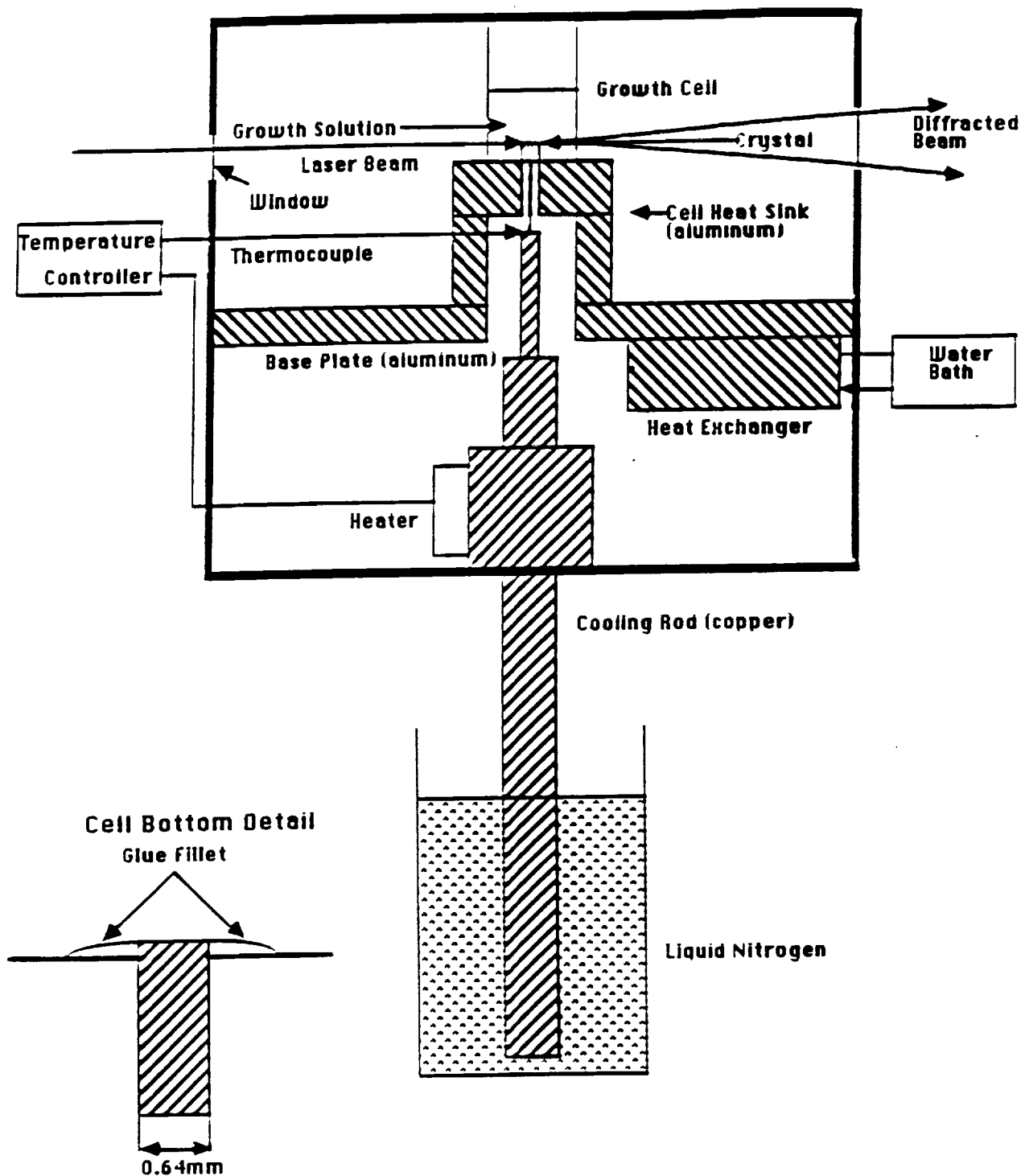
Fig. 9. Schematic of Thermonucleator.

A schematic drawing and photograph of the actual apparatus ("thermonucleator") used to induce localized supersaturation in a protein solutions are shown in Fig. 9 and 10 respectively. It consists of a sealed lucite box (~15 x 15 x 9") containing a glass growth cell (1 cm^2 ID x 4.5 cm), a heat exchanger connected to an external temperature controlled water bath, and a copper cold finger which protrudes up through the bottom of the growth cell (see detail in inset) and out the bottom of the lucite box into a dewar containing liquid nitrogen. A resistance heater and thermocouple are attached to the cold finger so that the surface temperature (T_S) in contact with the solution can be accurately controlled. In these preliminary experiments, the diameter of the cold finger protruding into the growth cell was 0.64 mm. The ambient temperature in the box (T_e) and, thereby, the bulk solution in the growth cell was controlled by the heat exchanger temperature. Both T_S and T_e can be programmed such that the supersaturation can be uniformly varied with time, but in the experiments described below, temperature was manually adjusted.

The procedure for nucleating a desired crystal is generally as follows: 1) The bulk solution is set at a near saturation (Fig. 8a). Under these stable conditions, critical size nuclei should not form. 2) T_S is adjusted so that the supersaturation is large enough to cause nucleation on the exposed surface of the cold finger (Fig.8b). The amount of undercooling should be such that the surface of the copper is at a temperature just inside the labile region described in Fig. 6. If the phase equilibria data (solubility) is not known, it is a rather simple matter to empirically find the appropriate temperature to cause nucleation to take place on the cold finger. 3) After solid forms on the tip, T_S (and sometimes T_e) is raised to try and dissolve all but a few of the crystallites which may form initially. In practice, this is difficult to achieve because it is hard to see very small crystallites in the growth cell. Laser light scattering techniques, when developed and incorporated into the system, should provide more control of this process. 4) After dissolving back the initial crystallites, T_S is decreased to that of the bulk solution, and 5) The temperature of both the bulk solution and the tip are slowly lowered to cause growth to take place on the existing seed or seeds (Fig. 8c).

The growth system is set up so that various diagnostic tools can be incorporated into the temperature controlled box, in the future, to monitor various aspects of the nucleation and growth process.

In this study, we report on preliminary results using the thermonucleator to control the nucleation and growth of ice, Rochelle salt, and lysozyme.
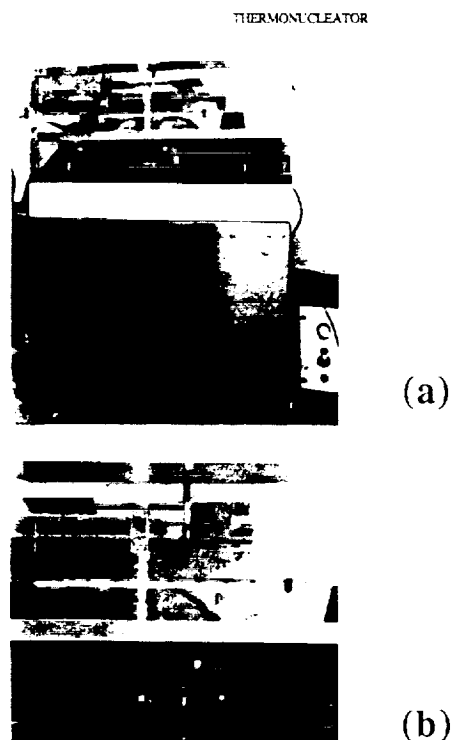
THERMONUCLEATOR

(a)

(b)

Fig. 10. a) Thermonucleator showing growth cell and cell heat sink (above base plate), and heat exchanger and cold spot temperature control (below base plate). The liquid nitrogen reservoir is in the base. 19.5"(h) x 15"(w), b) Close-up of growth cell, cell heat sink, control thermocouple (above base plate), heat exchanger, cold spot heater and air circulation fan.

solution was prepared by the method of Holden and Morrison.[14] The salt was dissolved in hot dionized water (1.3 gm/gm of water) and then cooled to 24°C so that the excess solute would precipitate, leaving a just saturated solution at that temperature. Using a hypodermic syringe fitted with a 0.22μ filler, 1-2 ml of the saturated solution was transferred to the growth cell.

For the lysozyme growth experiments, 74 mg of commercial material (Sigma) was dissolved in a 2 ml of buffer solution (0.1 M sodium acetate at pH 4.0) to give a concentration of 37 mg/ml. To this solution, 2% NaCl (20 mg/ml) was added. The solution was then transferred to the growth cell as described above. The solubility data used to adjust T_s and T_e was from Pusey.[15]

Temperature gradients in the growth cell were measured using a copper-constantan thermocouple (3 mil wire). The bare tip was supported by a 0.5 mm ID tube.

A Gyyr Time lapse video system was used to monitor and record the growth process and for extracting data on growth rates.

Ice-Water System

Figure 11 shows the lateral temperature variations in the growth cell containing de-ionized water as a function of height from the surface of the cold finger. The ambient temperature, T_e, of the bulk liquid was set at 25°C, while T_S was set to 15°C. It can be seen that the gradient decreases with distance away from the copper wire both laterally and vertically. The hemispherical isotherms are shown in Fig. 12. Note the end effect where the copper, glue, and bottom of the cell meet.

Fig. 11. Lateral temperature variations at various heights in growth cell. Ambient temperature (T_e) 25°C, Cold finger temperature (T_S) 15°C
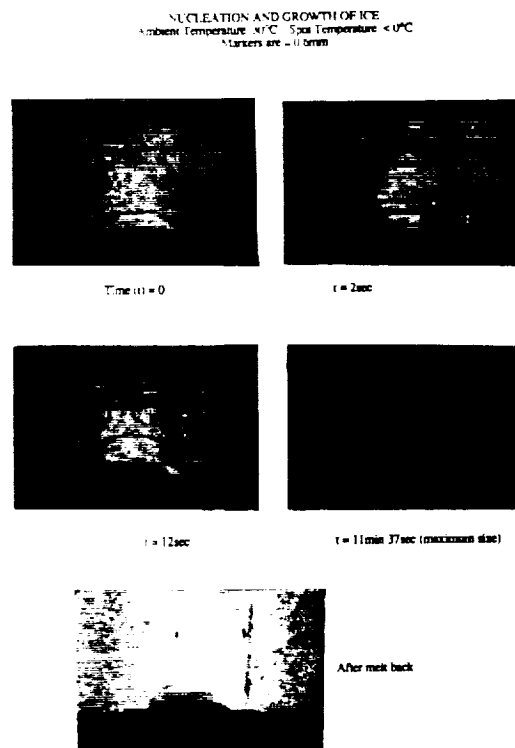

Fig. 12. Isotherms above cold finger. Ambient temperature (T_e) 25°C.

20

In the ice crystallization experiments, the ambient temperature was set at 30°C and T_s at the nominal freezing point of water, 0°C. Figure 13 is a sequence of photographs showing the growth of an ice crystal directly on the cold finger surface as a function of time. Note that the shape of the crystal mimics the shape of the isotherms shown in Fig. 12. Unlike the growth of Rochelle salt and lysozyme, the ice crystallization experiments are an example of melt growth. The liquid-solid growth interface of course represents the freezing point isotherm. The last frame in Fig. 13 shows that the process is reversible.

Fig. 13. Sequence of photographs showing the nucleation and growth of an ice crystal in the Thermonucleator.

Rochelle Salt

While the ice-water system was used to study the temperature profiles and temperature control aspect of the thermonucleator apparatus, Rochelle salt was used as a model material to study the nucleation and growth characteristics in a typical aqueous solution growth situation. Figure 14 shows a sequence of photographs taken from a time lapse video monitor. The solution initially saturated at 24°C was kept at 24°C in the

21

enclosure, while T_S was lowered to 16°C. The first frame shows a small single crystal growing directly on the copper and subsequent frames show the crystal growing. Between frames 2 & 3, and 3 & 4 T_e was manually lowered by 2°C each, causing the crystal to grow larger, with T_S allowed to reach T_e prior to cooling. A secondary crystallite can be seen growing to the right of the original crystal. It is not clear whether this crystal was present initially or nucleated at a later time but the former possibility is more likely. By programming the temperature at a slow, uniform rate, the size and quality of the crystal should be improved significantly.

Fig. 14. Sequence of photographs showing the nucleation and growth of Rochelle salt in the Thermonucleator.

Lysozyme

Lysozyme was used as a model system representative of the growth of biological macromolecules. The sequence of photographs shown in Fig. 15 represent the first attempt to nucleate a protein on the cold finger. Initially, T_e was set at 25°C and T_S at 15°C. Within approximately 4.5 hours, the first crystal of lysozyme could be observed. Three

crystallites can clearly be seen, even in the first photograph. After about 8 hours, T_S was allowed to equal T_e and T_e was kept constant for another 15 hours. During this period, several additional crystallites developed which can clearly be seen in the frame shot at 8:12 a.m. At this point, T_e was lowered in 2°C steps twice during a 26 hours period. One can see that under the cooling rate regime used, a cluster of crystals developed. However, the cluster lies exactly on the surface of copper cold finger.

Fig. 15. Sequence of photographs showing the nucleation and growth of lysozyme in the Thermonucleator.

In the latest lysozyme crystallization, the same crystallizing solution was used. The bulk temperature (T_e) was set at 22°C and the cold finger temperature (T_S) at 12°C. After 6.5 hrs, crystals appeared on the cold finger (Fig. 16) and T_e and T_S were adjusted to 20°C. Observation after an additional growth period of 15.5 hrs showed that there was a polycrystalline mass on the cold finger. The temperatures were raised (T_S to 28°C and T_e to 26°C) to dissolve all but a few of the crystals. When only a few crystals remained (after 7.5 hrs), the temperatures were lowered to continue the growth (T_e=21°C, T_S=20°C). The temperatures were lowered 2°C increments over the next few days as growth continued. The final temperatures were T_e =18°C and T_S =16°C. During this growth sequence (Fig. 16), one large (270μ) crystal and several smaller crystals were formed on the cold finger. The change in crystal size with time is plotted in Fig. 17. In spite of the cooling, the growth rate decreased, as shown in Fig. 18.
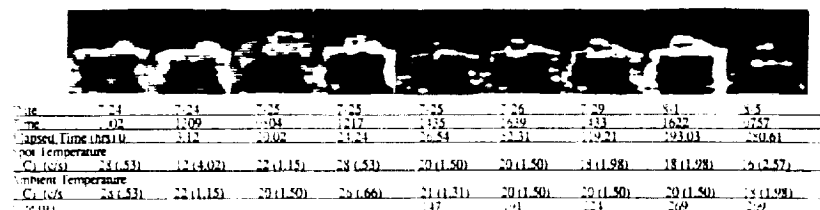
23

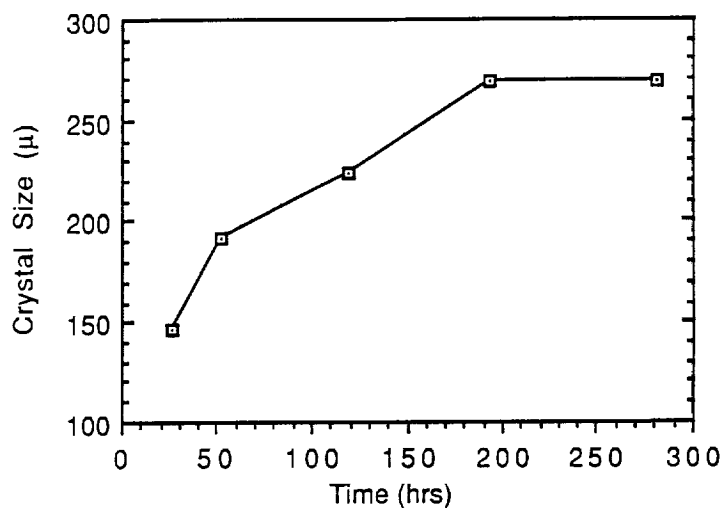Fig. 16. Photographs showing the results of the improved growth procedure for the growth of lysozyme.

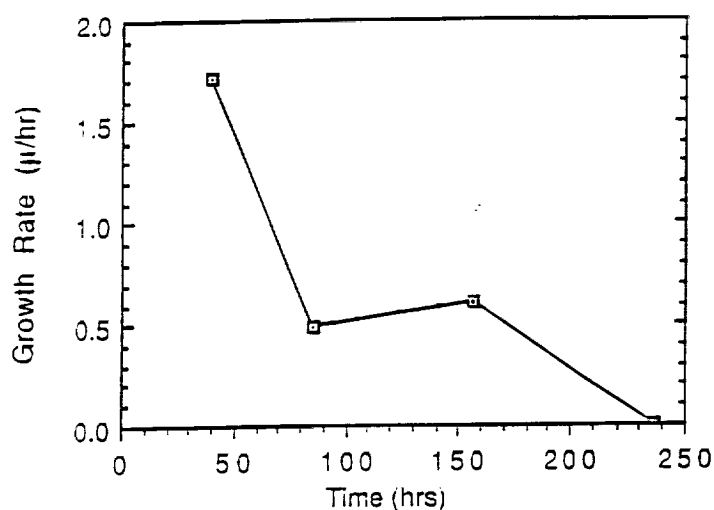Fig. 17. Crystal size vs. time for lysozyme crystal grown in latest experiment.

Fig. 18. Growth rate vs. time for the lysozyme crystal in Fig. 17.

24

SUMMARY

An apparatus has for the first time been designed and built to control supersaturation in a localized region of a bulk solution, thereby permitting a separation of the nucleation and growth processes. The effectiveness of this "thermonucleating" device has been demonstrated with the nucleation and growth of ice, Rochelle salt, and lysozyme. The method relies on the species to be grown having a temperature dependent solubility, but an alternative procedure could be devised to create the localized supersaturation by controlling composition in a small region of the solution. A more precise means of detecting nucleation must be developed to work in conjunction with localized supersaturation control.

IV. ISOCITRATE LYASE - GROWTH MORPHOLOGY

The successful results on the growth of isocitrate lyase (ICL) in recent space experiments led us to study the reasons for this dramatic improvement in crystal morphology and quality. Using the well known hanging drop method, ICL crystals grow with a "dendritic" morphology (Fig. 19) under 1-g conditions and as equi-axed crystals in μg. A series of experiments was designed to investigate the factors affecting the 1-g morphology of ICL crystals and to related the results to the μg experiments.
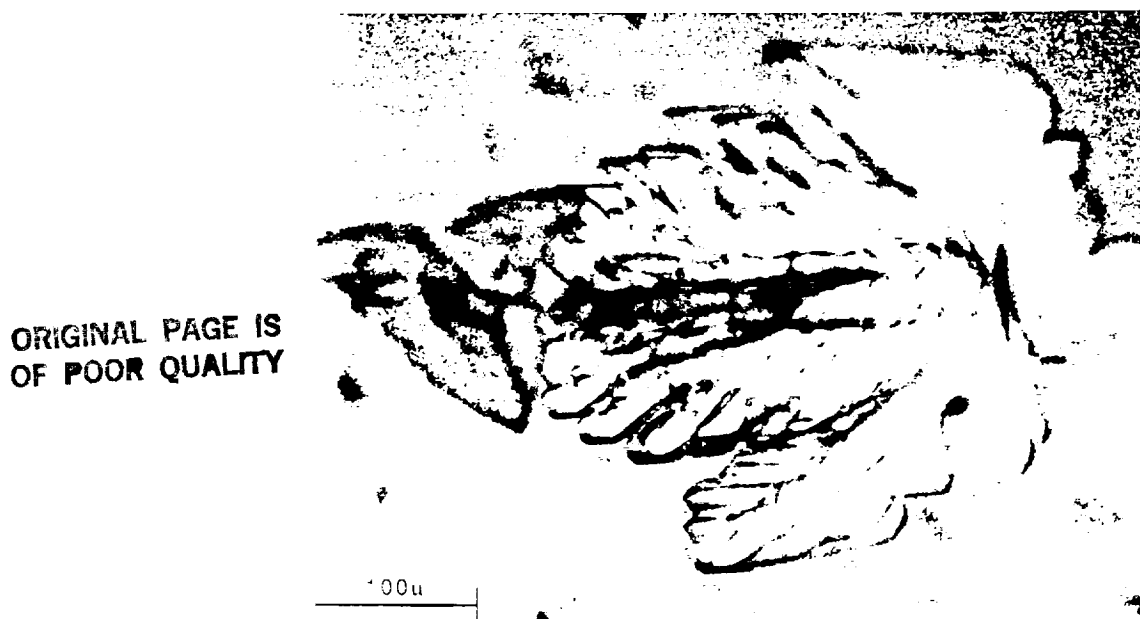
Fig. 19. Isocitrate lyase crystal (ICL) grown from 4μl hanging drop (ICL concentration 10mg/ml).

All of the ICL used in these experiments came from Du Pont Merck. Before use, the ICL solution (ICL in 0.1M Tris-HCl pH 7.8, 10mM EDTA, 1mM DTT, 0.4M KCl) was incubated at 4°C for 24 hrs with a reducing solution (0.3M Glutathione, 66mM EDTA in 1M Tris-HCl pH 8.0) (4:100 v/v) and an inhibitor solution (50mM 3-nitriproprionate, 0.5M MgOAc in 50mM Tris-HCl pH 7.0) (4:100 v/v). The ICL concentrations were 10mg/ml (Du Pont Merck) and 12mg/ml (Stanford). The well solution was 1.6-2.0M (60-80% saturation) Na-citrate (Na-cit). The usual drop size was 4μl (2μl ICL solution and 2μl well solution). Crystals appeared within one week at 24°C.

The source of the poor morphology was investigated by closely observing drops during crystallization. These 4μl hanging drops (12mg/ml ICL solution, 72% Na-Cit well solution) were observed through a microscope at 150x.

Figure 20 shows a typical result of the hanging drop experiments. It is obvious that the poor morphology results from uncontrolled growth originating at the corners of the crystal. Such growth can result from either excessive supersaturation[12] or from flow effects.[16] To attempt to separate these effects, a 1mm x 3mm cross section cell with glass walls was built to allow imaging of fluid flows. A 4μl ICL crystallizing solution was vapor equilibrated against Na-cit in the well of the cell. No flows were observed, but three crystals were found with a more regular morphology than had been previously seen (Fig. 21).
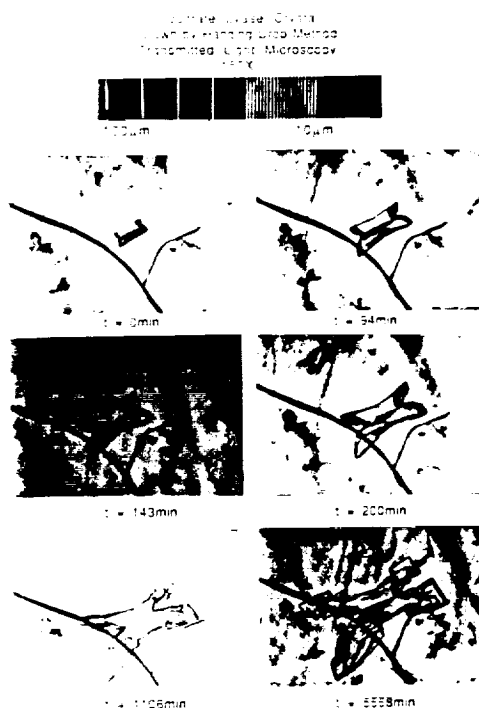
Fig. 20. Time lapse of ICL crystal grown from 4μl hanging drop (ICL concentration 12mg/ml).

effects.[16] To attempt to separate these effects, a 1mm x 3mm cross section cell with glass walls was built to allow imaging of fluid flows. A 4μl ICL crystallizing solution was vapor equilibrated against Na-cit in the well of the cell. No flows were observed, but three crystals were found with a more regular morphology than had been previously seen (Fig. 21).

The same growth experiment was repeated in 1.88mm diameter capillaries to better observe the crystals. The ICL crystals grown in the capillaries exhibited a very well formed morphology (Fig. 22). These crystals have been x-rayed at Du Pont and have the same space group ($P2_12_12_1$) and unit cell parameters (a=80.7Å, b=123.1Å, c=183.4Å) as the previously grown crystals. The "octagonal" cross section arises from the orthorhombic symmetry with the facets bounded by (100), (010) and (110) faces. The end of the crystals are bounded by either (001) (flat) or (101) (wedge shaped) faces.
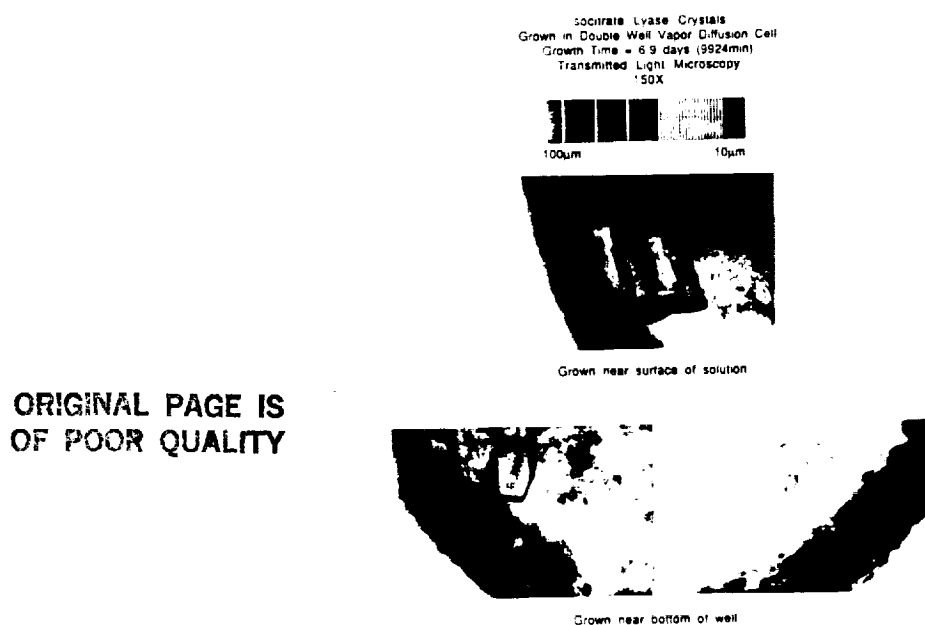
Fig. 21. ICL crystals grown in 1mm x 3mm cell (4µl of 12mg/ml).

A comparison of Figs. 20 & 22 shows that the initial breakdown in morphology occurs at the corners of the "octagonal" crystal. This breakdown is probably associated with excessive supersaturation and, thus, with unstable growth conditions.

(a)

(b)

Fig. 22. ICL crystals grown in 1.88mm capillary (12mg/ml) showing
a) flat termination by a (001) type face, and b) a wedged shaped
termination by (101) type face.

Sibille and his co-workers have developed mathematical models to describe the evaporation from both drops and capillaries in equilibrium with well solutions.[17,18] These models may be expressed in the general form as:

a) for the hanging drop

$$t / t = F[x(t)]$$

and b) for the capillary

$$t / t = G[\partial(t)]$$

where

$$x(t) = \frac{a(t)}{a_0}; V(t) = \Omega_v(\alpha)\, a(t)^3;\ \Omega_v(\alpha) = \frac{4}{3}\, \pi\, \cos^4(\frac{1}{2}\, \alpha)[\ 1+2\, \sin^2(\frac{1}{2}\, \alpha)]$$

where a is the contact angle of the drop, and

$$\partial(t) = \frac{\Delta_1(t)}{\Delta_1(0)};\ \Delta_1(t) = n_1(e)[t] - n_1(c)[t]$$

where $n_1(e)[t]$ is the number of moles of water in the crystallizing solution and $n_1(c)[t]$ the number of moles of water in the well. The characteristic times, t, for the two models are defined by:

a) for the hanging drop

$$\tau = \frac{3\, \Omega_v(\alpha)\, a_0{}^2\, n_1(b)\, R\, T}{\Omega_a(\alpha)\, D_1\, p_1^0\, w\, n_2(b)\, V_1};\ \Omega_a(\alpha) = 4\, \pi\, \cos^2(\frac{1}{2}\, \alpha)$$

and b) for the capillary

$$\tau = \frac{R\, T\, L\, \Delta_1{}^2(0)}{4S\, D_1\, p_1^0\, w\, n_2}$$

where $n_1(b)$ is the number of moles of water in the well, D_1 the diffusion coefficient of water in air, p_1^0 the vapor pressure of pure water, w the vapor pressure lowering constant, $n_2(b)$ the number of moles of precipitant in the well, V_1 the partial molar volume of water, L the distance between the crystallizing solution and the well, S the cross sectional area of the capillary, n_2 the total number of moles of precipitant in the crystallizing solution and the well, and R and T have their usual meaning. The parameters needed to use these models for ICL and lysozyme were calculated as outlined in ref.[17] The osmotic coefficient for Na-cit was estimated using equation 10, section 14 of Shoemaker and Garland.[19] The contact angle for the hanging drop simulations was 90°C, the well volume 500μl and the spacing 5mm. The well volume for the capillary simulations was 350μl and the spacing was 3.5cm. Figure 23 compares the results of applying these models to a drop and a

1.88mm ID capillary containing the same volume of ICL solution. The drop evaporates at a rate which is two orders of magnitude faster than the capillary. This difference in rates is consistent with laboratory observations.
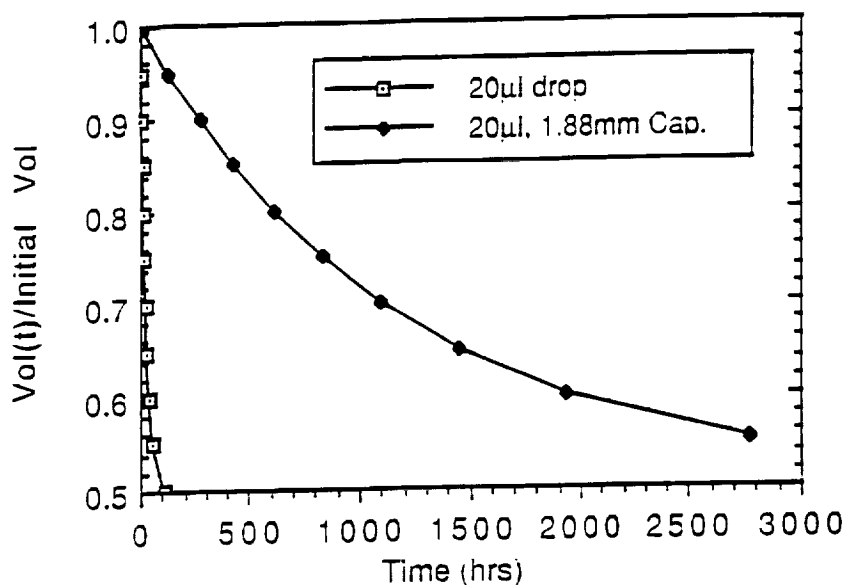

Fig. 23.   Volume ratio vs. time comparing 20μl drop with 20μl in a 1.88mm capillary. Simulates ICL crystallization.

The rate of change of supersaturation is somewhat more complicated than the change in volume since the concentration of both the crystallizing species and the precipitant change with the change in volume and, through the solubility curve, they both affect the supersaturation.. Unfortunately, the solubility curve of ICL is not known. In order to demonstrate the changes in supersaturation that occur during vapor equilibrium, the models were applied to lysozyme using the solubility data for lysozyme developed by Pusey.[15] Figure 24 shows the evaporation rate for lysozyme solutions which contain 30mg/ml lysozyme and 2% NaCl equilibrated against a well of 4% NaCl. The rate of change of supersaturation is shown in Fig. 25.

In an actual crystal growth experiment, the growing crystals would have an effect on the supersaturation of the solution. To illustrate this effect in a lysozyme solution, 10 crystals were assumed to nucleate at c/s = 4 (a value consistent with other studies). No further nucleation was allowed to take place. The crystals grew according to the kinetics determined by Pusey and Naumann[20] and the amount of lysozyme removed from solution during each growth period was determined. Figure 26 shows the results for both a hanging drop and a capillary. The supersaturation in the drop reaches a peak which is
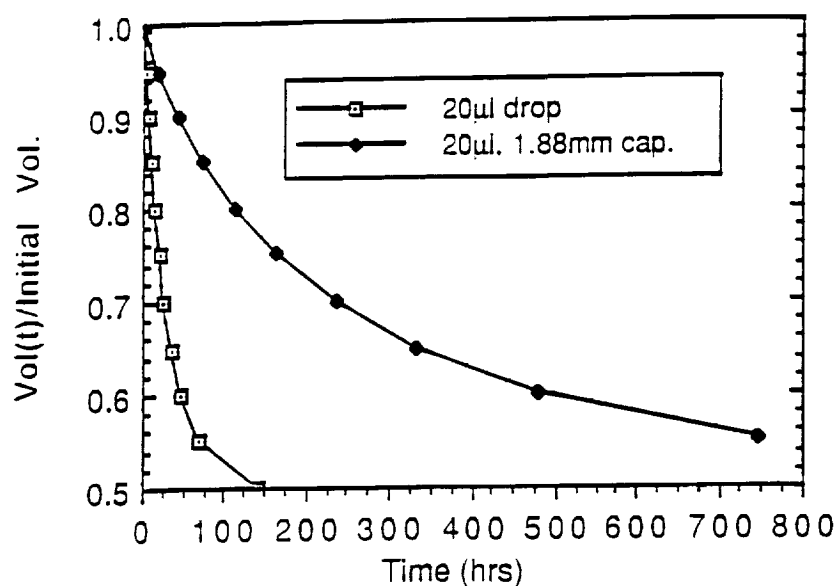
31

Fig. 24. Volume ratio vs. time comparing 20μl drop with 20μl in a
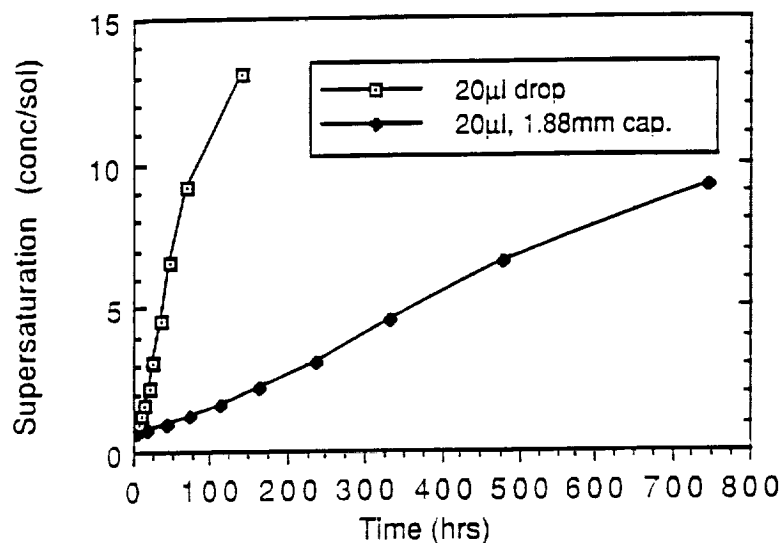1.88mm capillary. Simulates lysozyme crystallization.

Fig. 25. Supersaturation vs. time for lysozyme comparing 20μl drop with
20μl in 1.88mm capillary.

almost double that of the capillary. The crystallizing system can react to this stress by
either nucleating more crystals (secondary nucleation), increasing the growth rate to the
point of instability or a combination of the two. Lysozyme does the latter showing
secondary nucleation and surface roughening. ICL exhibits morphological instability.
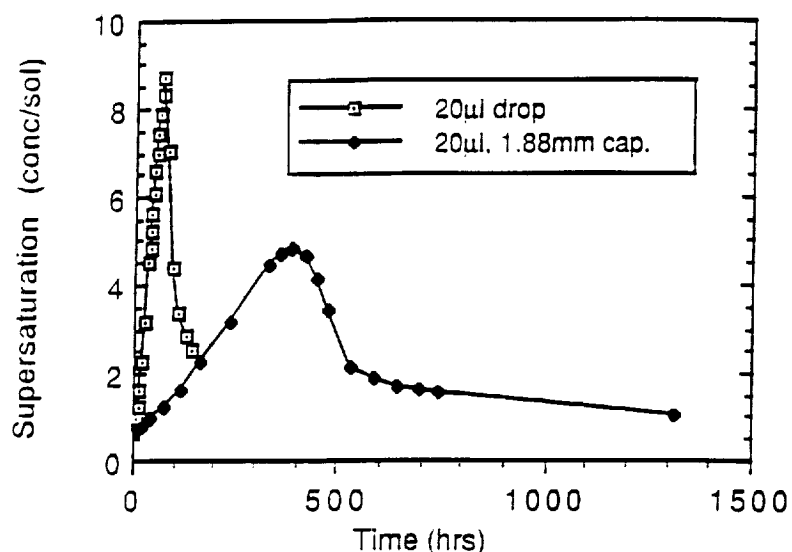
Fig. 26. Supersaturation vs. time for lysozyme comparing 20μl drop with
20μl in 1.88mm capillary. 10 crystals are nucleated at c/s = 4 and
allowed to grow.

Figure 27 shows an ICL crystal which was grown by Du Pont Merck in low-g
during a shuttle mission. The morphology is greatly improved over those grown by the
hanging drop technique on Earth. The drops used in space were larger (30μl vs. 4μl) than
those used on Earth which raises the question of whether the improvements in crystal
quality are related to the effects of μg or simply the difference in evaporation rate. Figure
28 shows the theoretical evaporation rates for 4μl and 30μl drops. The rate of equilibration
is 5x slower for the larger drop which, based on the results of the capillary experiments,
may explain the better morphology of the crystals grown in these drops.

There are other factors which may affect the space grown crystals. It has been
pointed out that drops evaporate slower than predicted in space due to the existence of a
concentrated layer of precipitant near the surface which lowers the vapor pressure of the
drop and retards evaporation.[21] This hypothesis was tested in the laboratory using
capillaries oriented so that the meniscus was at the top of the liquid column (meniscus up),
at the bottom (meniscus down) and with the meniscus vertical. A simulated ICL growth
(all components present except the protein) was done in these capillaries and the results are
shown in Fig. 29. The evaporation rate of the meniscus down capillary which will have a
concentrated layer of precipitant at the interface does appear to be slightly slower. In actual
ICL growth experiments, a precipitate layer appeared at the interface in the meniscus down
capillary. In some cases crystals eventually grew in this layer, but their morphology was
intermediate between the "octagonal" crystals and those grown in the hanging drop. The
existence of the precipitate acted to moderate the supersaturation in the same manner that the

growing crystals did in the lysozyme growth simulation. This mechanism may be operative during low-g hanging drop growth and can explain the type of crystals seen in the ICL experiments.
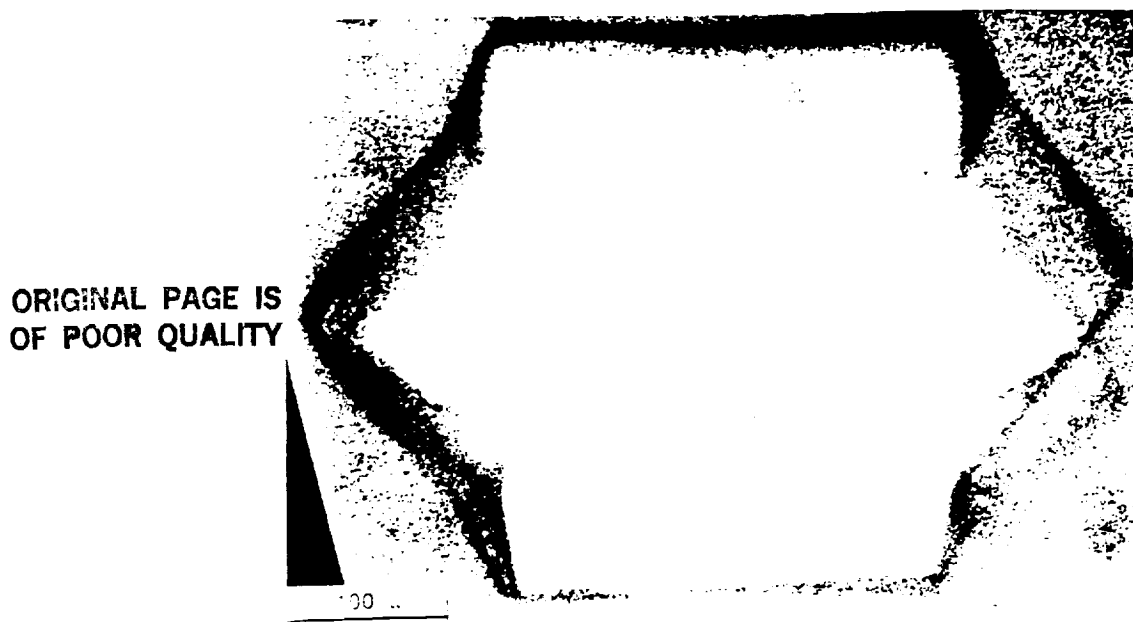

ORIGINAL PAGE IS
OF POOR QUALITY

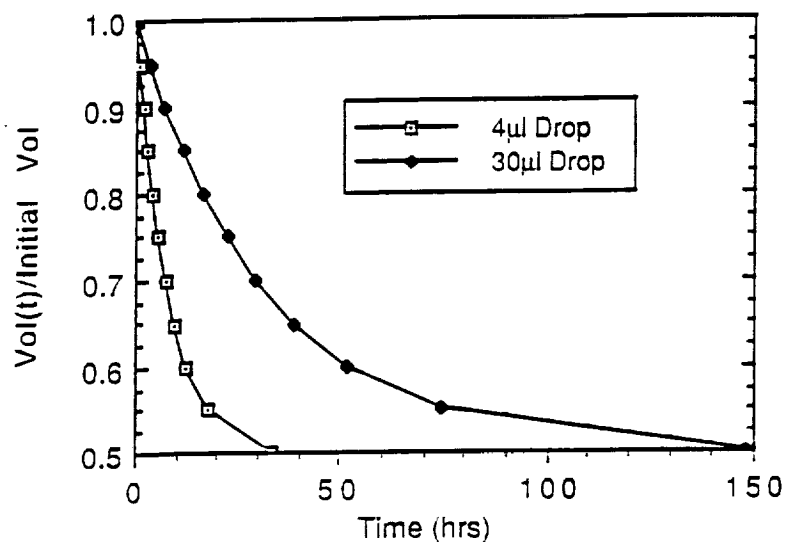Fig. 27. ICL crystal grown from 30μl drop (10mg/ml) in μg.

Fig. 28. Volume ratio vs. time comparing 4μl drop with a 30μl drop. Simulates ICL growth.
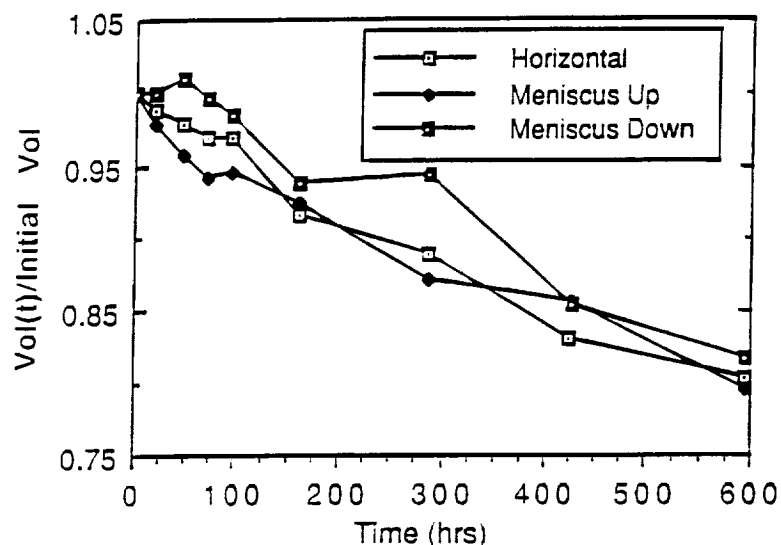
34

Fig. 29. Volume ratio vs. time for capillaries with the meniscus oriented in different directions.

The "octagonal" ICL crystals were grown in the meniscus up configuration. The horizontal configuration yields small, needle-like ICL crystals which appear to be of the "octagonal" type. These results indicate that some degree of mixing is desirable in the growth of ICL from capillaries.

The poor morphology of the ICL crystals grown by the hanging drop method in 1-g was due to high (unstable) growth rates due to high supersaturation. While it is necessary in all unseeded "batch" type crystal growth to increase the supersaturation high enough to cause nucleation, a slower rate of increase of the supersaturation does lead to more controlled growth and crystals with better morphology. This effect is further mitigated by the presence of growing crystals or a precipitate both of which will act to lower the overall supersaturation. The slow rate of supersaturation can be achieved by using vapor diffusion equilibration in small diameter capillaries. An alternative approach which is potentially more controllable is to use the method proposed by Wilson and co-workers[22] in which flowing nitrogen of controlled humidity controls the rate of evaporation.

The ICL growth experiments conducted in the capillaries indicate that some convective mixing is beneficial to the crystal growth by providing mixing and a uniform supersaturation in the crystallizing solution. Pusey and co-workers[23] have demonstrated in the case of lysozyme that high flow rates can cause cessation of growth. However, most small molecule aqueous crystal growth is done with some form of stirring (see i.e.

Buckley[24] and Chernov[12]). The best crystals will be expected to be found between the extremes of no flow (mixing) and rapid flows which can cause cessation of growth in protein systems.

The usual flows found in protein crystallization are due to solutal convection where gravity acts on density differences at the growth interface or at the vapor-liquid interface where evaporation is taking place. These flows can be non-uniform and unpredictable. The capillary experiments with ICL may have been fortuitous in that the size of the capillary and the volume of solution may have provided a Grashof number which yielded a suitable flow regime for growth. It is possible to engineer growth systems to give the proper Grashof number if the parameters of the system are known. However, the need to quantify the parameters can be by-passed by using gravity as a variable. To date this parameter has been explored only at the limits available: 1-g and µg. Experiments in an induced artificial gravity between the extremes are needed to study the effect of gravity and flow on the growth and morphology of protein crystals.

SUMMARY

The studies with ICL highlight the importance of the effect of growth rate on crystal quality. This will be a new area of emphasis in this research program. A plan is being developed to study the effect of growth rate not only on macro-defects such as external morphology, but also on micro-defects which can reduce x-ray diffraction resolution of the crystals. Techniques will be developed to reduce these defects.

V. REFERENCES

1. A. McPherson, Preparation and Analysis of Protein Crystals, Wiley (1982).

2. H. A. Meirs and F. Issac, *Proc. Roy. Soc.* A79, 322 (London) (1907).

3. E. I. Givargizov, Oriented Crystallization on Amorphous Substrates, Plenum Press, NY (1990).

4. A. McPherson and P. Shlichta, *J. Crystal Growth* 85, 206 (1987).

5. A. McPherson and P. Shlichta, *J. Crystal Growth* 90, 44 (1988).

6. A. McPherson, Preparation and Analysis of Protein Crystals, Wiley (1982).

7. M. F. Gulyi, L. V. Gudkova, R. G. Deghtyar, N. I. Mironenko, and N. V. Latyshko, *Doklady of USSR Acad. Sci.* 225, 211 (in Russian) (1975).

8. R. C. DeMattei and R. S. Feigelson, *J. Crystal Growth* 97, 333 (1989).

9. E. I. Givargizov and A. B. Limanov, *Microelectronic Eng.* 8, 273 (1988).

10. V. I. Klykov and N. N. Sheftal, 52, 687 (1987).

11. R. S. Feigelson, *J. Crystal Growth* 90, 1 (1988).

12. A. A. Chernov, Modern Crystallography III: Crystal Growth (Springer-Verlag, New York, 1984).

13. R. C. DeMattei and R. S. Feigelson, J. Crystal Growth 110, 34-40 (1991).

14. A. Holden and P. Morrison, Crystal and Crystal Growing, The MIT Press, Cambridge, MA, 02142 (1982).

15. E. Cacioppo, S. Munson, and M. L. Pusey, J. Crystal Growth 110, 66 (1991) and, E. Cacioppo and M. L. Pusey, submitted to J. Crystal Growth.

16. R.-F. Xiao, J. I. D. Alexander and F. Rosenberger, private communication.

17. L. Sibille and J. K. Baird, *J. Crystal Growth* 110, 72 (1991).

18 L. Sibille, J. C. Clunie and J. K. Baird, *J. Crystal Growth* 110, 80 (1991).

19. D. P. Shoemaker and C. W. Garland, Experiments in Physical Chemistry, McGraw-Hill, New York (1962).

20. M. Pusey and R. Naumann, *J. Crystal Growth* 76, 593 (1986).

21. W. W. Fowlis, L. J. DeLucas, P. J. Twigg, S. B. Howard, E. J. Meehan, Jr., and J. K. Baird, *J. Crystal Growth* 90, 117 (1988).

22. L. J. Wilson, T. L. Bray and F. L. Suddath, *J. Crystal Growth* 110, 142 (1991).

23. M. Pusey, W.K. Witherow and R. Naumann, *J. Crystal Growth* 90, 105 (1988).

24. H.E. Buckley, Crystal Growth, John Wiley and Sons, New York (1951).